GROWTH AND CHARACTERIZATION OF NANOSTRUCTURED NICKEL OXIDE THIN FILMS FOR PHOTODETECTION APPLICATIONS

ANAS AWAD HASAN AHMED

UNIVERSITI SAINS MALAYSIA

2020

GROWTH AND CHARACTERIZATION OF NANOSTRUCTURED NICKEL OXIDE THIN FILMS FOR PHOTODETECTION APPLICATIONS

by

ANAS AWAD HASAN AHMED

Thesis submitted in fulfilment of the requirements for the degree of Doctor of Philosophy

July 2020

DEDICATION

I dedicate this work to the soul of my father may Allah Almighty grant him

Al Jannah (Ameen)

ACKNOWLEDGEMENT

First and foremost, all praise is for Almighty Allah for granting me health, patience and strength to carry out this research.

I would like to express my deepest gratitude to my main supervisor Dr. Marzaini Rashid and my co-supervisor Prof. Dr. Md. Roslan Hashim for their invaluable guidance and support to achieve outstanding goals in this research work. Thank you Dr. Marzaini Rashid and Prof. Md. Roslan Hashim for having your doors open every time I needed help. Without your advice and comments this work would not be possible.

I would also like to acknowledge Taiz University for providing me a PhD scholarship to carry out this work. A great appreciation and acknowledgement also go to Nano-optoelectronic Research Laboratory (NOR Lab) and Solid-State laboratory staff for their technical support during conducting experiments and characterization. My heartfelt gratitude also goes to my family members: to my mother and my wife for their prayers and encouragement.

TABLE OF CONTENTS

ACKNOWLEDGEMENT ii

TABLE OF CONTENTS iii

LIST OF TABLES viii

LIST OF FIGURES x

LIST OF ABBREVIATIONS xv

LIST OF SYMBOLS xvi

ABSTRAK xviii

ABSTRACT xx

CHAPTER 1 INTRODUCTION 1

1.1 Introduction to NiO 1

1.2 Problem Statement 2

1.3 Research Objectives 4

1.4 Thesis Originality 4

1.5 Thesis Outlines 5

CHAPTER 2 LITERATURE REVIEW AND THEORY 7

2.1 Introduction 7

2.2 Crystal Structure of NiO 7

2.3 Growth of NiO Thin Films by Magnetron Sputtering: Review 9

2.3.1 Growth of NiO Thin Films at Different Oxygen Partial Pressures 9

2.3.2 Growth of NiO Thin Films at Different Substrate Temperatures 11

2.3.3 Growth of NiO Thin Films at Different RF Powers 13

2.3.4 Growth of NiO Thin Films at Different Film Thicknesses 14

2.4 Principle of Magnetron Sputtering 17

2.4.1 Radio frequency Sputtering 17

2.5 Growth of NiO Thin Films by Spin Coating: Review 18

2.6 Principle of Sol Gel Spin Coating 23

2.7 Review of Photodetectors based on NiO Thin Films.................................. 24

2.8 Theoretical concepts of Photodetectors 28

2.8.1 Metal-Semiconductor-Metal Contact 30

2.8.2 Photoelectric Characteristics 34

2.8.2(a) Responsivity 34

2.8.2(b) Photo-to-Dark Current Ratio (PDCR)............................ 34

2.8.2(c) Rise Time and Fall Time.. 35

2.8.2(d) Dependence of Photocurrent on Power Density 36

2.9 Summary 37

CHAPTER 3 METHODOLOGY AND CHARACTERIZATION TECHNIQUES 38

3.1 Introduction 38

3.2 Cutting and Cleaning of Substrates 38

3.3 Deposition of NiO Thin Films by Non-Reactive RF sputtering. 40

3.3.1 Deposition of NiO Thin Films at Different Substrate Temperatures 41

3.3.2 Deposition of NiO Thin Films at Different RF Sputtering Powers 42

3.3.3 Deposition of NiO Thin Films at Different Film Thicknesses…………………………………………………............ 42

3.4 Growth of NiO Thin Films by Sol-gel Spin Coating Technique 44

3.4.1 Growth of Spin Coated NiO Thin Films at Different Growth Parameters 45

3.5 Characterization Facilities.. 48

3.5.1 Field Emission Scanning Electron Microscopy............................. 48

3.5.2 Atomic Force Microscopy 50

3.5.3 X-ray Diffraction 51

3.5.4 UV-Vis Reflectance Spectroscopy ... 53

3.6 Fabrication and Characterization of Multi-wavelength Photodetectors ... 56

CHAPTER 4 RESULTS AND DISCUSSION GROWTH OF NANOSTRUCTURED NiO THIN FILMS ON SILICON SUBSTRATE BY RADIO FREQUENCY MAGNETRON SPUTTERING ... 59

4.1 Introduction ... 59

4.2 Growth and Characterizations of Nanostructured NiO Thin Films on Si Substrate at Different Substrate Temperatures ... 59

4.2.1 Surface Analysis ... 59

4.2.1(a) Morphology Analysis ... 60

4.2.1(b) Surface Roughness Analysis ... 61

4.2.2 Structural Characterization ... 63

4.2.3 Elemental Analysis ... 69

4.2.4 UV-Vis Reflectance Analysis ... 70

4.2.5 Summary ... 71

4.3 Growth and Characterizations of Nanostructured NiO Thin Films on Si Substrate at Different RF Powers ... 72

4.3.1 Surface Analysis ... 72

4.3.1(a) Morphology Analysis ... 72

4.3.1(b) Surface Roughness Analysis ... 74

4.3.2 Structural Characterization ... 76

4.3.3 Elemental Analysis ... 80

4.3.4 UV-Vis Reflectance Analysis ... 80

4.3.5 Summary ... 82

4.4 Growth and Characterizations of Nanostructured NiO Thin Films on Si Substrate at Different Thicknesses ... 82

4.4.1 Surface Analysis ... 82

4.4.1(a) Morphology Analysis ... 82

4.4.1(b) Surface Roughness Analysis 84

4.4.2 Structural Characterization 86

4.4.3 Elemental Analysis 88

4.4.4 UV-Vis Reflectance Analysis 89

4.4.5 Summary 90

4.5 Summary 91

CHAPTER 5 RESULTS AND DISCUSSION GROWTH OF NANOSTRUCTURED NiO THIN FILMS ON SILICON SUBSTRATE BY SOL-GEL SPIN COATING TECHNIQUE 93

5.1 Introduction 93

5.2 Sol-Gel Growth and Characterization of Nanostructured NiO Thin Films on Si Substrate at Different Molar Ratios of Diethanolamine 93

5.2.1 Surface Analysis 94

5.2.1(a) Morphology Analysis 94

5.2.1(b) Surface Roughness Analysis 97

5.2.2 Structural Characterization 99

5.2.3 Elemental Analysis 101

5.2.4 UV-Vis Reflectance Analysis 101

5.2.5 Summary 102

5.3 Sol-Gel Growth and Characterization of Nanostructured NiO Thin Films on Si Substrate at Different Annealing Temperatures 103

5.3.1 Surface Analysis 103

5.3.1(a) Morphology Analysis 103

5.3.1(b) Surface Roughness Analysis 106

5.3.2 Structural Characterization 108

5.3.3 Elemental Analysis 111

5.3.4 UV-Vis Reflectance Analysis 112

5.3.5 Summary 114

5.4 Sol-Gel Growth and Characterization of Nanostructured NiO Films on Si Substrate at Different Precursor Molarities 114

5.4.1 Surface Analysis 114

5.4.1(a) Morphology Analysis 114

5.4.1(b) Surface Roughness Analysis 117

5.4.2 Structural Characterization 119

5.4.3 Elemental Analysis 123

5.4.4 UV-Vis Reflectance Analysis 124

5.4.5 Summary 125

5.5 Summary 126

CHAPTER 6 RESULTS AND DISCUSSION NANOSTRUCTURED NiO THIN FILMS GROWN OVER SILICON SUBSTRATE AS MSM MULTI-WAVELENGTH PHOTODETECTOR 128

6.1 Introduction 128

6.2 Photoelectric Characteristics 128

6.2.1 Current-voltage (I-V) Characteristics 129

6.2.2 Responsivity 138

6.2.3 Photo-to-Dark Current Ratio (PDCR) 142

6.2.4 Rise and Fall Time 146

6.2.5 Influence of Light Intensity on Photocurrent 150

CHAPTER 7 CONCLUSIONS AND FUTURE WORK 153

REFERENCES 155

LIST OF PUBLICATIONS

LIST OF TABLES

Page

Table 2.1 Fundamental properties of NiO 8

Table 2.2 Previous studies reported on the deposition of NiO films using sputtering technique. 16

Table 2.3 Growth of spin coated NiO films on different substrate at different growth conditions. 22

Table 2.4 A summary of Photodetectors based on NiO grown over Si substrate 27

Table 4.1 Structural parameters of NiO films deposited at different substrate temperatures. 68

Table 4.2 Atomic percentage of Ni and O content in NiO films at different substrate temperatures. 70

Table 4.3 Structural parameters of NiO films at different RF sputtering power. 77

Table 4.4 Elemental composition of NiO films grown at different RF powers. 80

Table 4.5 Structural parameters of NiO films at different film thicknesses. 88

Table 4.6 Elemental composition of NiO films grown at different RF powers 88

Table 4.7 A summary of NiO results obtained using non-reactive RF sputtering. 92

Table 5.1 Structural parameters of nanostructured NiO films coated at different DEA:NiAc molar ratios. 100

Table 5.2 Elemental composition of NiO thin films grown at various DEA: NiAc molar ratios. 101

Table 5.3 Structural parameters of NiO films annealed at different temperature 110

Table 5.4 Atomic percentage of Ni and O content in NiO films annealed at different temperatures in atmospheric air. 112

Table 5.5 Structural parameters of nanostructured NiO films grown at different precursor molarities. 122

Table 5.6 Elemental composition of NiO films grown at different molarities.. 123

Table 5.7 A summary of the results of spin coated NiO films grown at different growth conditions... 127

Table 6.1 A comparison of the responsivity of the photodetectors under illumination with different wavelengths at 5 V. 142

Table 6.2 A comparison of the PDCR values of the photodetectors at different wavelengths.. 145

Table 6.3 Photocurrent of the photodetectors at applied voltage of 5 V... 146

Table 6.4 A summary of rise time and fall time of photodetectors under light illumination with different wavelengths at bias 5 V... 148

LIST OF FIGURES

Page

Figure 2.1 Unit cell structure of NiO. 8

Figure 2.2 Schematic of magnetron sputtering process. 18

Figure 2.3 Geometry and bias of a typical photodetector. 29

Figure 2.4 Schematic of energy-band diagram of MSM contact (a) Energy-band diagram in thermal equilibrium (b) Energy-band diagram under bias (c) Electric field under bias (d) Flat-band voltage and its corresponding electric field (e). 32

Figure 2.5 I-V characteristic of a typical Si photodetector under dark condition. 33

Figure 2.6 Rise time and fall time estimation of a photodetector. 36

Figure 3.1 Flowchart of synthesis, characterization and MSM photodetector application of NiO thin films. 39

Figure 3.2 (a) RF magnetron sputtering system (b) Si substrates fixed on substrate holder. 41

Figure 3.3 Flowchart of optimizing the deposition parameters of RF sputtered NiO thin films. 43

Figure 3.4 Spin coating system (Model: MTI VTC-100B). 44

Figure 3.5 Flowchart of optimizing the growth parameters of spin coated NiO thin films. 47

Figure 3.6 Schematic diagram of growth process of NiO thin film. 48

Figure 3.7 (a) A photo of FESEM instrument used in this study (b) Schematic of principle of FESEM. 50

Figure 3.8 (a) A photograph of AFM unit (b) Illustration of principle of AFM. 51

Figure 3.9 (a) A photograph of X-ray diffractometer (b) Bragg's condition (c) Diffraction of X-ray from a crystallite. 53

Figure 3.10 (a) A photograph of UV-Vis spectrometer (b) Schematic illustration of the UV-Vis system. 55

Figure 3.11 (a) Schematic diagram of the finger mask (b) and (c) Photos of bare Si and NiO/Si PDs, respectively (d) Schematic diagram of the measurement setup of photodetection properties. 58

Figure 4.1 FESEM micrographs showing surface morphology of NiO thin films deposited at different substrate temperatures. 61

Figure 4.2 AFM images of NiO films deposited at (a) RT (b) 100 ^{o}C (c) 200 ^{o}C (d) 300 ^{o}C. 62

Figure 4.3 Surface roughness of NiO films at different substrate temperatures. 63

Figure 4.4 (a) XRD patterns of NiO films at RT and 100 ^{o}C (b) XRD pattern of NiO film at 200 ^{o}C (c) XRD Pattern of NiO film at 300 ^{o}C (d) Variations in intensity and FWHM of NiO with substrate temperature. 66

Figure 4.5 (a) Full scale UV-Vis reflectance spectra and (b) Enlarge UV-Vis spectra of NiO films at different substrate temperatures 71

Figure 4.6 FESEM images of NiO films grown at different RF sputtering powers 73

Figure 4.7 3D AFM images of NiO films grown at (a) 150 W, (b) 200 W, (c) 250 W, (d) 300 W. 75

Figure 4.8 RMS surface roughness values of NiO films at different RF powers. 75

Figure 4.9 XRD patterns of NiO films grown at different RF powers. 76

Figure 4.10 Deposition rate as a function of the RF power 79

Figure 4.11 UV-Vis reflectance spectra of NiO films grown at different RF powers 81

Figure 4.12 Surface morphology of nanostructured NiO films grown at different thicknesses and at fixed substrate temperature and RF power of 100 ^{o}C and 200 W, respectively. 83

Figure 4.13 AFM images of NiO films grown at (a) 350 nm (b) 640 nm (c) 920 nm (d) RMS surface roughness values versus thickness. 85

Figure 4.14 XRD spectra of NiO films grown at various thicknesses. 87

Figure 4.15 UV-Vis spectra of NiO films grown at various thicknesses. 90

Figure 5.1 Low magnification FESEM micrographs of NiO films coated at different DEA to nickel acetate molar ratios. 95

Figure 5.2 High magnification FESEM images of NiO films coated at different DEA to nickel acetate molar ratios..................................96

Figure 5.3 3D AFM images of NiO films coated at different DEA:NiAc molar ratios...98

Figure 5.4 RMS surface roughness values of NiO films coated at different DEA:NiAc molar ratios..99

Figure 5.5 XRD patterns of NiO coated at different values of molar ratio. 100

Figure 5.6 UV-Vis reflectance spectrum of NiO film grown at DEA:NiAc molar ratio of 1:1..102

Figure 5.7 FESEM micrographs of NiO thin films post annealed at different temperatures. 105

Figure 5.8 AFM images of As-coated NiO film and NiO films annealed at different temperatures. 107

Figure 5.9 RMS surface roughness values of NiO films annealed at different annealing temperatures...108

Figure 5.10 XRD patterns of NiO films annealed at various annealing temperatures...109

Figure 5.11 Crystallite size of (200) plane and FWHM as a function of annealing temperature. 111

Figure 5.12 UV-Vis reflectance spectra of as-coated and annealed NiO films at different annealing temperatures.....................................113

Figure 5.13 The energy band gap of NiO films annealed at different temperatures. 113

Figure 5.14 FESEM micrographs of NiO films grown at different precursor molarities...116

Figure 5.15 AFM images of NiO films grown at different precursor molarities..118

Figure 5.16 RMS surface roughness values of nanostructured NiO films as a function of precursor molarity. 119

Figure 5.17 XRD patterns of NiO films grown at different precursor molarities..120

Figure 5.18 UV-vis reflectance spectra of NiO films grown at different precursor molarities....124

Figure 5.19 Energy band gap of NiO films grown at different precursor molarities....125

Figure 6.1 I-V characteristics of MSM n-Si PD in the dark and under illumination with different wavelengths 130

Figure 6.2 UV-Vis reflectance spectra of bare Si, the optimal RF sputtered and spin coated NiO films. 131

Figure 6.3 I-V characteristics of MSM RF sputtered NiO film/n-Si PD in dark and under illumination with different wavelengths. 132

Figure 6.4 I-V characteristics of MSM spin coated NiO film/Si PD in dark and under illumination with different wavelengths for (a) whole scan range (b) enlarged range. 134

Figure 6.5 Schematic diagram illustrating photodetection mechanism of NiO film grown on Si substrate (a) Energy band diagram of NiO/Si heterostructure (b) Incident UV light with energy higher than the energy band gap of NiO (c) Incident Vis-NIR light with energy lower than the band gap of NiO. The bend lines show the electric field direction....136

Figure 6.6 Responsivity of Si, RF-sputtered NiO/Si and spin-coated NiO/Si PDs as a function of applied voltage at light intensity of 1.4 mW/cm^2 under illumination with (i) 365 nm light, (ii) 625 nm light and (iii) 850 nm light....140

Figure 6.7 Responsivity of Si, RF-sputtered NiO/Si and spin-coated NiO/Si PDs as a function of the wavelength at light intensity of 1.4 mW/cm^2 and bias voltage of 5 V. 142

Figure 6.8 PDCR of Si, RF-sputtered NiO/Si and spin-coated NiO/Si PDs as a function of applied voltage at light intensity of 1.4 mW/cm^2 under illumination with (i) 365 nm light, (ii) 625 nm light and (iii) 850 nm light. 144

Figure 6.9 Transient photocurrent response of MSM PDs at 5 V under (a) 365 nm light, (b) 625 nm light and (c) 850 nm light. 147

Figure 6.10 Rise time and fall time of the PDs upon exposure to (a) 365 nm light, (b) 625 nm light and (c) 850 nm light. 149

Figure 6.11 Transient photocurrent response of RF-sputtered NiO/Si and spin-coated NiO/Si PDs at different light intensities under (a) 365 nm light (b) 625 nm light (c) 850 nm light....151

Figure 6.12 Fitting curves of photocurrent versus incident light intensity of RF-sputtered NiO/Si and spin-coated NiO/Si PDs under (a) 365 nm light (b) 625 nm light (c) 850 nm light. 152

LIST OF ABBREVIATIONS

a. u.	Arbitrary unit
AC	Alternating current
AFM	Atomic force microscopy
C.B	Conduction band
DC	Direct current
DEA	Diethanolamine
EDX	Energy dispersive X-ray spectroscopy
eV	Electron volt
FESEM	Field emission scanning electron microscopy
FWHM	Full width at half maximum
I-V	Current-Voltage
MSM	Metal-semiconductor-metal
NiAc	Nickel acetate tetrahydrate
NIR	Near infrared
PD	Photodetector
PDCR	Photo-to-dark current ratio
RF	Radio frequency
RMS	Root mean square
RT	Room temperature
SCCM	Standard cubic centimeters per min
UV	Ultraviolet
V.B	Valence band
V_{FB}	Flat band voltage
Vis	Visible
XRD	X-ray diffraction

LIST OF SYMBOLS

A	Ampere
A	Area
a	Lattice constant
Å	Angstrom
Ar	Argon
c	Speed of light
D	Crystallite size
d	Interplanar spacing
e	Charge of electron
E	Electric field
E_F	Fermi level
E_g	Energy band gap
h	Planck's constant
I	Current
I_d	Dark current
I_{ph}	Photocurrent
L	Inter-electrode spacing
M	Molarity
n	Diffraction order
Ni	Nickel
O	Oxygen
^oC	Degree Celsius
P_{in}	Optical power
P_λ	Light intensity
R	Responsivity
Si	Silicon

T	Absolute temperature
V	Voltage
V_b	Built-in barrier
V_F	Forward voltage
V_R	Reverse voltage
W	Depletion region
W	Watt
β	Full width at half maximum
ε	Lattice strain
θ	Bragg’s angle
λ	Wavelength
ν	Frequency
Ω	Ohm
Φ_n	Barrier height

PERTUMBUHAN DAN PENCIRIAN STRUKTUR NANO TIPISAN NIPIS NIKEL OKSIDA UNTUK APLIKASI FOTOPENGESAN

ABSTRAK

Tujuan kajian ini adalah untuk menumbuhkan tipisan nipis Nikel Oksida (NiO) dengan kualiti kehabluran yang baik ke atas substrat Si untuk aplikasi fotopengesan. Kajian ini dibahagikan kepada tiga bahagian utama. Bahagian pertama memberi tumpuan kepada pertumbuhan struktur nano tipisan nipis NiO dengan menggunakan teknik percikan RF. Analisis XRD menunjukkan bahawa kualiti kehabluran telah bertambah baik dengan meningkatkan suhu substrat dari suhu bilik hingga 100 ^{o}C; walau bagaimanapun, tipisan nipis NiO telah diuraikan menjadi logam Ni pada suhu substrat 300 ^{o}C. Dengan peningkatan kuasa RF dari 150 hingga 300 W dan ketebalan tipisan nipis dari 350 hingga 640 nm, kehabluran tipisan nipis NiO dipertingkatkan, diikuti oleh degradasi dengan peningkatan dalam kuasa dan ketebalan kepada 300 W dan 920 nm masing-masing. Tipisan nipis NiO yang dienapkan pada 100 ^{o}C, kuasa RF 200 W dan ketebalan 640 nm menunjukkan kualiti kehabluran optimum yang kemudiannya dipilih untuk aplikasi fotopengesan. Bahagian kedua kajian ini mengkaji pertumbuhan struktur nano tipisan nipis NiO menggunakan teknik salutan putaran sol-gel. Tipisan nipis NiO yang ditumbuhkan pada nisbah molar penstabil sebanyak 0:1 mengalami retakan yang teruk. Peningkatan nisbah molar kepada 1:1 menghilangkan retakan. Dengan meningkatkan suhu penyepuhlindapan dari 300 ^{o}C hingga 650 ^{o}C, saiz hablur dan kekasaran permukaan tipisan nipis meningkat, sementara jurang jalur tipisan nipis menurun. Dengan peningkatan kemolaran prekursor (dari 0.1 hingga 0.9 M), saiz hablur meningkat (dari 18.94 hingga 34.54 nm). Tipisan nipis NiO

melalui salutan putaran sol-gel dengan 0.9 M, nisbah molar penstabil 1:1 dan disepuhlindap pada 600 ^{o}C menunjukkan kualiti terbaik dan ia dipilih untuk aplikasi fotopengesan. Bahagian ketiga menyiasat potensi sifat fotopengesanan panjang gelombang berbilang fotopengesan (PD) logam-semikonduktor-logam (MSM) berdasarkan tipisan nipis yang tumbuh. Hasilnya menunjukkan peningkatan dalam prestasi fotopengesanan bagi NiO PD percikan RF dan NiO PD salutan putaran berbanding dengan MSM Si PD. Responsiviti dan nisbah arus foto kepada arus gelap bagi NiO PD percikan RF dan NiO PD salutan putaran adalah lebih tinggi daripada Si PD dengan faktor 3.65, 14.6 dan 31 dan 303, masing-masing di bawah pendedahan kepada (jarak gelombang) 365 nm.

GROWTH AND CHARACTERIZATION OF NANOSTRUCTURED NICKEL OXIDE THIN FILMS FOR PHOTODETECTION APPLICATIONS

ABSTRACT

The aim of this study was to grow good crystalline quality of NiO thin films over Si substrate for photodetection application. The study was divided into three main parts. The first part focuses on growth of nanostructured NiO thin films using non-reactive RF sputtering technique. XRD analysis showed that with increasing substrate temperature from RT to 100 ^{o}C, the crystallite size was increased from 19.14 to 28.20 nm; followed by a decrease to 14.71 nm as the substrate temperature was increased to 200 ^{o}C. The further increase of the temperature to 300 ^{o}C, resulted in decomposition of NiO film into Ni. With the increase of the RF power from 150 to 200 W and the film thickness from 350 to 640 nm, the crystallite size was improved from 17.46 to 28.20 nm and from 28.20 to 29.66 nm, respectively; however, the crystalline quality of the films was degraded when the RF power and film thickness were further increased to 300 W and 920 nm, respectively. NiO film deposited at 100 ^{o}C, RF power 200 W and thickness 640 nm showed optimal crystalline quality with crystallite size value of 29.66 nm for which it was then selected for photodetection application. The second part of this work studies the growth of nanostructured NiO films using sol-gel spin coating technique. NiO film grown at stabilizer molar ratio of 0:1 suffered from severe cracks. The increase in the molar ratio to 1:1 resulted in cracks-free film. NiO film coated at molar ratio of 1:1 was annealed at different temperatures (300 to 650 ^{o}C). With the increase of the annealing temperature, the surface roughness and the crystallite size of the films were increased from 1.07 to 5.72

nm and from 12.79 to 37.31 nm, respectively. Whereas, the energy band gap of the films was decreased from 3.81 to 3.45 eV. With increasing precursor molarity from 0.1 to 0.9 M, the crystallite size was increased from 18.94 to 34.54 nm, while the band gap was decreased from 3.85 to 3.31 eV. Sol-gel spin coated NiO film with 0.9 M, stabilizer molar ratio 1:1 and annealed at 600 ^{o}C revealed the best crystalline quality with crystallite size of 34.54 nm and it was chosen for photodetection application. The third part investigates the potential multi-wavelength photodetection properties of metal-semiconductor-metal (MSM) photodetectors (PDs) based on the grown films. The results revealed an enhancement in the multi-wavelength photodetection performance of RF sputtered NiO PD and spin coated NiO PD as compared to MSM Si PD. The responsivity of RF sputtered NiO/Si PD was higher than that of Si PD by factor of 3.56 and 1.34 under light illumination with wavelengths of 365 and 625 nm, respectively, whereas it showed same responsivity under exposure to 850 nm. Spin coated NiO/Si PD revealed much higher responsivity relative to Si PD. The responsivity was higher than that of Si PD by a factor of 14.60, 2.70 and 2.11 for wavelengths of 365, 625 and 850 nm, respectively. The photo-to-dark current ratio of RF sputtered NiO/Si and spin coated NiO/Si PDs were remarkably increased as compared to Si PD with a factor of 97, 35 and 27 and 946, 172 and 137 upon light exposure to 365, 625 and 850 nm wavelengths, respectively. All the photodetector showed fast response with rise time and fall time < 0.3 s.

CHAPTER 1

INTRODUCTION

1.1 Introduction to NiO

Transition metal oxide nanostructures (TMONs) can be defined as materials in which a transition metal (M: Zn, Cu, Ni, Ti, etc.) reacts with oxygen to form a binary compound (M-O). Over the past years, TMONs have been investigated widely due to their high importance in electrical, magnetic and optical applications. In general, nanostructures are known as materials that have at least one dimension in the range of 1-100 nm. Accordingly, nanostructures can be classified based on their dimensionality into three types: zero-dimensional (0D), one-dimensional (1-D) and two-dimensional (2-D) nanomaterials. By scaling down the dimensions of the nanostructures into nano-size, the electronic structures can be altered which in turn leads to manipulation in the properties of those nanostructured materials [1].

Nickel oxide (NiO) nanostructure is among other TMONs that has attracted considerable attention worldwide due to its remarkable properties, such as nontoxicity, excellent chemical stability, high transparency and desirable electrical and optical properties [2-4]. Unlike most of transparent TMONs, which are n-type semiconductors in their nature, NiO is known as a p-type semiconductor with a wide energy band gap in the range of 3.2-3.8 eV [5]. Accordingly, NiO films are of a great interest to be utilized as, UV light functional layer, electron blocking layer and hole transport layer in optoelectronic devices [6-9]. In addition, NiO can be used as antiferromagnetic layer in spin valve films due to its antiferromagnetic properties [10]. Stoichiometric (defect-free) NiO is an insulator at room temperature because of its high resistivity (higher than 10^{13} Ω.cm) [11]. However, the prepared NiO films always deviate from this ideality due to the formation of microstructure defects such as, nickel vacancies and

interstitial oxygen atoms, which bring about a reduction in the resistivity as well as giving rise to p-type conductivity in NiO films [12].

Preparation of NiO thin films with nano-size structure plays a vital role in the variety of applications, especially those which depend on the interaction with the surrounding ambient, namely, catalysis, solar cells, gas sensors and photodetectors. In this kind of applications, the nanostructured morphology is a key issue in improvement of the performance of devices, whereby the high effective surface area of nanostructures enhances the reactivity of the surface of interest with the surrounding environment due to the availability of more active sites which results in better performance. NiO nanostructures can be synthesized in different shapes like, nanowires [13], nanosheets [14], nanorod [15] and nanoparticles [16-19] using various chemical and physical synthesis techniques such as electrospinning, hydrothermal, chemical bath deposition, sol-gel spin coating, pulsed laser ablation, electron beam deposition, spray pyrolysis and magnetron sputtering deposition. Among these techniques, RF sputtering and spin coating are useful techniques to prepare nanostructured NiO thin films on large scale of substrates with very good homogeneity as compared with other techniques.

1.2 Problem Statement

Growth of good crystalline quality of nanostructured NiO thin films is of great importance in many applications. For instance, in photodetectors, dark current is a figure of merit parameter to evaluate the performance of the photodetector, whereby obtaining low dark current is a prerequisite for fabricating photodetectors with high performance. The dark current of any photodetector is affected by the crystalline quality of the sensing layer. Low crystalline quality implies the formation of high

density of intrinsic defects such as O interstitials and Ni vacancies which in turn lead to increase the charge carriers and then the dark current increases. In addition, poor crystalline quality indicates the existence of more grain boundaries that hinder the carriers transport which adversely affect the speed of the photodetector.

Due to the need for growth of good crystalline quality NiO films for photodetector application, it is important to consider the parameters that influence the crystalline quality of the films. Among those parameters, the type of the substrate over which the sensing layer is grown. It has been reported that the films grown over glass substrate suffer from poor crystalline quality as compared to the films grown over silicon substrate due to the amorphous nature of the glass [20-22]. Therefore, silicon is the best choice to serve as substrate for growth of good crystalline quality NiO films owing to its high crystalline quality and its lattice structure is same as that of NiO (FCC structure). Based on the literature review, there is a lack of studies reported on the influence of the deposition parameters on the structural properties of NiO thin films grown over Si substrate using sputtering technique. Further, the reported studies on NiO films grown over Si substrate were conducted in oxygen reactive sputtering in which O reacts with Ni to form NiO films which leads to form poor crystalline quality films due to the non-ideal reactivity between O and Ni [23-25]. Investigation of the properties of NiO films grown over Si substrate using non-reactive sputtering, in which NiO film is deposited from NiO target in pure Ar environment without presence of oxygen gas, is beneficial for obtaining good crystalline quality of NiO films. However, non-reactive RF sputtering technique has some limitation related to the non-availability of oxygen and fixed composition of the starting material (NiO target). Therefore, cost-effective sol-gel spin coating technique can be introduced to grow NiO films over Si substrate with more flexibility in the growth parameters. In addition,

there are no studies reported on growth of NiO films on Si substrate using cost-effective sol-gel spin coating technique at different molarities and different annealing temperatures.

1.3 Research Objectives

The main objectives of this thesis can be summarized as follows;

1. To investigate the crystalline quality of nanostructured NiO thin films deposited on Si substrate at different deposition parameters by using non-reactive sputtering technique.
2. To evaluate the crystalline quality of nanostructured NiO thin films grown over Si substrate at different growth parameters using sol-gel spin coating technique.
3. To investigate the potential of grown NiO films over Si substrate as MSM multi-wavelength photodetectors.

1.4 Thesis Originality

Owing to the importance of growth of nanostructured NiO films with good crystalline quality for photodetection application, this study was conducted with the aim of growing high crystalline quality of NiO thin films over silicon substrate using two different techniques which are non-reactive RF sputtering and sol-gel spin coating. To obtain high crystalline quality films, various parameters were explored and the films with the best crystalline quality were selected to serve as sensing layer for photodetection application. Two MSM photodetectors based on non-reactive RF sputtering and spin coating techniques were fabricated and their photodetection properties were compared with each other and with that of bare Si photodetector as

well. Some novel results were obtained in this study for first time and they are highlighted as follows;

1. The decomposition of non-reactive RF sputtered NiO thin film into metallic nickel upon increasing the substrate temperature up to 300 ^{o}C.
2. Growth of nanostructured NiO thin films with good crystalline quality over Si substrate at different precursor molarities using sol-gel spin coating technique.
3. Fabrication of multi-wavelength planar MSM photodetector based on NiO/Si heterostructure. NiO acts as sensing layer under illumination with UV light due to its wide bandgap and it serves as antireflection layer to enhance the absorption of visible and near infra-red light in Si substrate through scattering of the light into the underlying Si substrate.

1.5 Thesis Outlines

This work contains seven chapters. Chapter 1 of this study includes a background about nanostructured NiO thin films. It also describes the existing problem in preparation of good crystalline quality of NiO films. Moreover, the research objectives of this study and the novel outcomes are highlighted in this chapter.

Chapter 2 presents the crystalline structure of NiO and its properties. It also provides literature review of growth of NiO thin films using reactive sputtering (DC sputtering), RF sputtering and sol-gel spin coating techniques. In addition, the principle of growing NiO thin films using magnetron sputtering and spin coating techniques are described. Literature review of photodetector based on NiO films as well as the theoretical concept of photodetectors are presented in this chapter.

The experimental procedure of the growth of NiO thin films and the characterization tools used to investigate the physical properties of the films are discussed in chapter 3.

Chapter 4 includes the results and discussion on the growth and characterization of nanostructured NiO thin films using non-reactive RF sputtering technique. The influence of changing the substrate temperature, RF power and film thickness on the morphological, structural and optical properties of NiO thin films is investigated.

In chapter 5, nanostructured NiO thin films grown by sol-gel spin coating technique are discussed and characterized using various characterization techniques. The physical properties of the films are investigated upon changing the stabilizer molar ratio, post-annealing temperature and precursor molarity.

Chapter 6 includes investigation on the potential multi-wavelength photodetection properties of metal-semiconductor-metal (MSM) photodetectors (PDs) based on bare Si substrate, RF sputtered NiO film/Si heterostructure and spin coated NiO film/Si heterostructure under illumination with UV, red and infra-red lights. The photodetection parameters such as, I-V characteristics, responsivity, photo-to-dark current ratio, rise time and fall time of the photodetectors are studied and compared with each other.

The conclusions of this research and the recommended future work are summarized in chapter 7.

CHAPTER 2

LITERATURE REVIEW AND THEORY

2.1 Introduction

This chapter is divided into two parts; In the first part, a short introduction about the crystal structure of NiO is presented. A literature review of growth of NiO thin films under different deposition parameters such as, substrate temperature, sputtering power and film thickness using direct current sputtering (DC sputtering) and radio frequency (RF) sputtering techniques is discussed. In addition, the effect of the growth parameters such as post-annealing temperature and the precursor molarity on the growth of NiO films is reviewed. This part also provides a review of using NiO thin films in photodetection application. In the second part, the fundamental principles of metal-semiconductor-metal contact and photodetectors are described.

2.2 Crystal Structure of NiO

Nickel oxide is an inorganic binary compound belonging to transition metal oxide materials. It exists in different oxidation states (different phases) such as Ni_2O_3 [26], Ni_3O_4 [27], NiO_2 [28] and NiO. However, the first three abovementioned phases are thermally and chemically unstable, therefore, they are not of researchers' interest. NiO is an intrinsic p-type semiconductor with face centred cubic (FCC) structure (NaCl like structure) in which Ni^{2+} and O^{2-} ions are arranged alternatively to form NiO as shown in Figure 2.1. Table 2.1 shows the fundamental properties of NiO. According to joint committee on powder diffraction standards (JCPDS), NiO is given card number of 00-047-1049 with diffraction peaks of 37.24°, 43.27°, 62.87°, 75.41° and 79.40° which correspond to (111), (200), (220), (311) and (222) lattice planes, respectively. Accordingly, the lattice constant value can be calculated using Bragg's law as 4.177 Å.

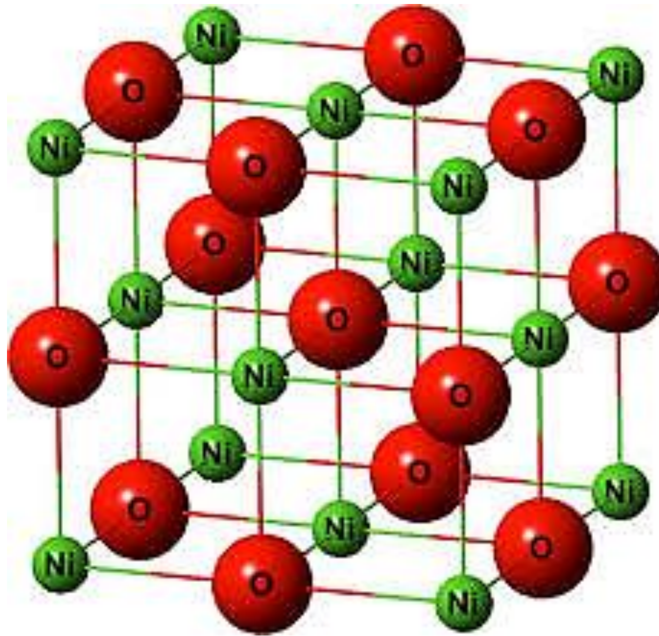

Figure 2.1. Unit cell structure of NiO [29].

Table 2.1: Fundamental properties of NiO [19]

Chemical formula	NiO
Structure	Face-centred Cubic
Lattice parameter	4.177 Å
Space group	Fm-3m
Molar mass	74.69 g/mol
Density	6.67 g/cm^3
Melting point	1,955 ^oC
Band gap	3.1-3.8 eV
Refractive index	2.18

2.3 Growth of NiO Thin Films by Magnetron Sputtering: Review

Magnetron sputtering technique has attracted tremendous attention of researchers worldwide to synthesize semiconductor thin films over large scale of substrates with good homogeneity and quality. It is a low cost and low temperature technique to grow good quality of NiO thin films as compared with MBE and MOCVD synthesis techniques [30, 31]. The growth of NiO thin films can be obtained either in reactive sputtering environment in which oxygen as reactive gas is introduced into the sputtering chamber or in non-reactive sputtering environment (only argon gas is used as plasma source). More details about the classification and the working principle of sputtering technique are given in section 2.4.

The literature review of growth of NiO thin films showed that magnetron sputtering technique has been reported to grow NiO thin films over different substrates. The growth of NiO thin films through magnetron sputtering technique can be controlled by various deposition parameters such as, the partial oxygen pressure, substrate temperature, sputtering power and film thickness, etc.

2.3.1 Growth of NiO Thin Films at Different Oxygen Partial Pressures

Seo and co-workers [32] deposited polycrystalline NiO thin films from Ni target by DC magnetron reactive sputtering at different oxygen content in the gas mixture of Ar and O_2. They found that on increasing the oxygen content from 3% to 20 %, the diffraction peak of (220) plane was shifted to higher 2θ angle which implied the increase of the strain effect due to the increase of nickel vacancies as the oxygen content was increased.

Soo Kim *et al*. [33] prepared polycrystalline NiO thin films on SiO_2/Si substrate by RF reactive sputtering of Ni target in a mixture of Ar and O_2 gas environment. The

films showed poor crystalline quality especially with increasing the oxygen content. By increasing the oxygen content from 30% to 100%, the diffraction peaks of (111) and (200) planes were shifted towards lower 2θ angles which was originated from the increase in the lattice constant due to the creation of more Ni vacancies.

Wang *et al*. [34] deposited NiO thin films from Ni target over glass substrate using DC reactive sputtering at different oxygen partial pressures. The films showed poor crystalline quality which was attributed to the formation of Ni vacancies as a result of the excess of oxygen content in the films. In addition, structural and XPS analysis revealed the existence of metallic Ni in the films prepared at lower values of oxygen partial pressure.

Chen and his group [35] deposited polycrystalline NiO thin films on glass substrate through non-reactive and reactive RF sputtering of NiO target in Ar and O_2 gas mixture. The structural properties of the films were investigated upon changing the O_2 partial pressure from 0% to 100%. They found that the NiO film deposited in pure Ar ambient (0% of O_2 partial pressure) has good crystalline quality as compared with the films deposited in a mixture of Ar and O_2 ambient. The lattice constant was calculated to increase from 4.25 to 4.30 Å when the O_2 partial pressure was increased from 0 to 100%. Such an increase in the lattice constant was ascribed to the creation of O interstitial atoms which led to the expansion of the lattice parameter of NiO films.

Domínguez-Cañizares *et al*. [25] prepared NiO thin films over Si substrate through non-reactive and reactive RF sputtering of NiO target in pure Ar and Ar + O_2 gas mixture. The study showed that NiO film grown in pure Ar ambient has good crystallinity with crystallite size of 18 nm; however, when 10% of O_2 gas was introduced to the plasma, the crystallite size was drastically decreased to 6 nm,

indicating deterioration of the crystallinity of the films due to the presence of oxygen that induced lattice disorder.

Zhao and co-workers [24] deposited NiO thin films on Si substrate from NiO target using non-reactive and reactive RF sputtering at different O_2 partial pressures (0, 20, 40, 60 and 80%). All NiO films exhibited preferred orientation in the (200) plane. The films prepared at partial pressure of 60 and 80% showed cracked surface morphology. The energy band gap of the films was decreased from 3.80 to 3.25 eV upon increasing the O_2 partial pressure from 0 to 80%. Such a decrease in the band gap resulted from the formation of non-stoichiometric defects (Ni vacancies and/or O interstitials). Based on the survey of literature review, it can be concluded that the growth of NiO thin films in presence of O_2 gas as reactive gas or plasma source adversely affects the crystalline quality of NiO thin films due to the formation of nickel vacancies and/or interstitial oxygen defects.

2.3.2 Growth of NiO Thin Films at Different Substrate Temperatures

Ai *et al*. [23] deposited NiO thin films over Si substrate from Ni target in Ar and O_2 environment through RF reactive sputtering at different substrate temperatures. They found that the films prepared at RT and 100 ^oC are amorphous; however, when the substrate temperature was increased to 200 ^oC the film showed small diffraction peak belonging to (200) plane. The further increase in the temperature to 400 ^oC resulted in change of the orientation growth from (200) to (111) plane. They attributed the change in the orientation to the presence of sufficient active oxygen species due to the decomposition of O_2 gas at elevated temperature which promotes the growth along (111) plane.

Kang and his group [36] prepared polycrystalline NiO thin films on SiO_2/Si substrate at substrate temperature varied from room temperature (RT) to 250 ^{o}C using RF sputtering technique. The films were prepared from Ni target in a mixture of Ar (75%) and O_2 (25%) gas. The structural analysis revealed an improvement in the crystalline quality of the films upon increasing the substrate temperature from RT to 250 ^{o}C. The lattice constant was decreased from 4.36 to 4.21 Å, whereas the crystallite size was increased from 6.2 to 10.5 nm.

The influence of substrate temperature on the structural properties of NiO thin films grown on sapphire substrate was also reported by Zhang and co-workers [37]. They found that the crystallinity of sputtered NiO films was improved with increasing the substrate temperature from 30 to 200 ^{o}C; however, the crystallinity was deteriorated when the temperature was further increased to 300 ^{o}C, suggesting the decomposition of NiO. The improvement in the crystallinity was assigned to the reduction in native defects (oxygen interstitial and nickel vacancies) as a result of the enhancement in the reactivity between Ni and active oxygen species when the temperature was increased from 30 to 200 ^{o}C.

Similarly, Jamal *et al*. [38] studied the effect of substrate temperature on the structural properties of NiO thin films. The films were prepared on glass substrate from NiO target in pure Ar environment using RF magnetron sputtering. They reported that by increasing the temperature from RT to 100 ^{o}C, the crystallite size was slightly increased (from 18 to 19.43 nm), followed by a decrease to 13.10 nm with increasing the temperature to 400 ^{o}C, indicating the degradation in crystalline quality of the films due to the decomposition of NiO.

2.3.3 Growth of NiO Thin Films at Different RF Powers

The influence of changing the sputtering power on the growth of NiO thin films was reported in the literature by different authors. The study conducted by Ryu and co-workers investigated the effect of RF power change (from 40 to 100 W) on the growth direction of NiO thin films over Si substrate [39]. NiO target was used as a raw material and the sputtering process was carried out in pure Ar and O_2 gases, separately. They discovered that the films grown in pure Ar gas exhibited only (200) diffraction peak. The peak appeared at RF power of 60 W and increased rapidly with increasing the power to 100 W which is an indication of growth of oriented NiO film with high crystallinity. In contrast, the films grown in pure O_2 gas showed only one diffraction peak along (111) plane. However, this peak appeared at power of 80 W and increased slightly with increasing the power to 100 W, indicating poor crystallinity.

Chen *et al.* [40] investigated the orientation growth of NiO thin films upon changing the RF sputtering power from 20 to 100 W. The films were grown over Si substrate through sputtering of Ni target in Ar and O_2 ambient. They found that the orientation growth was changed from (200) to (111) plane as the RF power was increased from 60 to 100 W which was attributed to the increase of the deposition rate.

Zhao and his group also prepared (200) oriented NiO films on Si substrate at RF power varied from 80 to 160 W. The deposition process was conducted by using NiO target as a raw material in a mixture of Ar and O_2 gas (1:1). The crystallinity of the films was improved by increasing the sputtering power to ~120 W, followed by degradation when the power was increased to 160 W [41]. Overall, all films showed poor crystalline quality as a result of the presence of oxygen gas.

Lu *et al*. [42] showed that by increasing the RF reactive sputtering power from 100 to 200 W, the crystallinity of NiO films grown on glass substrate was systematically decreased, whereas the film deposited at 200 W showed very weak signal of (200) diffraction plane. In addition, a small peak belonging to (111) metallic Ni was observed at 200 W.

2.3.4 Growth of NiO Thin Films at Different Film Thicknesses

Chen *et al*. [43] employed RF sputtering technique to synthesize NiO thin films at different film thicknesses in pure O_2 gas environment. The films were deposited using NiO target as the starting material on glass substrate. The study revealed that the crystallite size was increased from 11 to 15 nm as the thickness was increased from 50 to 100 nm, followed by a decrease of crystallite size to 12 nm with increasing the thickness to 150 nm. The further increase in the film thickness to 300 nm resulted in increasing the crystallite size to 14 nm. They assigned the decrease in the crystallite size to the formation of new smaller crystallites over the bigger ones.

Another study on the dependence of the structural properties of NiO thin films upon change of the film thickness was achieved by Reddy and co-workers [44]. The films were grown over glass substrate through DC reactive sputtering in Ar and O_2 gas mixture. It was observed that the crystallite size of (200)-textured NiO films was increased from 8.23 to 21.09 nm when the thickness was varied from 150 to 250 nm. However, the further increase in the film thickness to 550 adversely affected the crystalline quality of the films, whereby the crystallite size was reduced to 4.15 nm. The lattice constant was reduced from 4.25 to 4.22 Å as the thickness was varied from 150 to 250 nm, followed by an increase to 4.28 Å upon increasing the film thickness to 550 nm.

On the other hand, it was reported in literature that by increasing the thickness of NiO, the crystallite size was improved [45, 46]. Keraudya *et al*. [45] grew NiO thin films on glass substrate at thicknesses varied from 50 to 1000 nm using DC reactive sputtering. They noticed that the films prepared at thickness of 50 and 100 nm are amorphous. On increasing the thickness from 300 to 1000 nm, the crystallite size and the lattice constant of (200) preferred orientation were increased from 15 to 25 nm and from 4.38 to 4.40 Å, respectively. Yilmaz with his group prepared NiO thin films over Si substrate at thicknesses 190 and 300 nm using RF reactive sputtering in Ar and O_2 ambient. The films showed poor crystallinity with crystallite size of 5.15 and 6.42 nm for the films prepared at 190 and 300 nm, respectively [46].

Table 2.2 summarizes reported studies in the literature on the deposition of NiO thin films at different substrate temperatures using reactive and non-reactive sputtering techniques. As shown, there was a lack of studies reported on non-reactive sputtered NiO films over Si substrate. In addition, there was a lack of the information available on the crystalline quality in terms of FWHM or crystallite size, indicating that more studies on the influence of substrate temperature on the structural properties of NiO films grown on Si substrate using non-reactive sputtering is of interest. Such kind of studies were conducted in our work and new findings were reported and published.

Table 2.2: Previous studies reported on the deposition of NiO films using sputtering technique.

Deposition method	Target	Ar/O_2 (%)	Sub. Temp. range (°C)/ Power (W)	Substrate type	Preferred Orientation	Crystallite size (nm)	Ref.
Reactive RF sputtering	NiO	0/100	250 – 400/ 50	Glass	(111)	_____	[47]
Reactive RF sputtering	NiO	0/100	RT – 350/ 150	Glass	(111) – (200)	11.4 – 18.1	[48]
Reactive RF sputtering	Ni	40/60	RT – 400/ 250	n-Si (100)	(200) – (111)	_____	[23]
Reactive RF sputtering	NiO	0/100	RT – 400/ 200	Glass	(111) – (200)	_____	[49]
Non-reactive RF sputtering	NiO	100/0	RT – 350	Glass	Poly – (200)	_____	[50]
Reactive DC sputtering	Ni	_____	30 – 450/ 150	Glass	(200) – (220)	28 – 20	[51]
Reactive DC sputtering	Ni	75/25	30 – 400/ 100	Glass	(200) – (220)	6.1 – 10.3	[52]
Reactive RF sputtering	Ni	20/80	RT – 250/ 200	SiO_2/Si	(200) – (111)	6.2 – 10.5	[36]
Reactive RF sputtering	NiO	50/50	30 – 600/ 100	Sapphire	(111)	____	[53]
Reactive DC sputtering	Ni	75/25	30 – 300/ 75	Sapphire	(111)	____	[37]
Non-reactive RF sputtering	NiO	100/0	RT – 400/ 50	Glass	(200) – (111)	13.1 – 19.4	[38]
Reactive DC sputtering	Ni	50/50	26 – 300/ 50	n-Si (100)	(111)	___	[54]

2.4 Principle of Magnetron Sputtering

Magnetron sputtering is a physical vapour deposition (PVD) method which is used to deposit a variety of materials (metals, semiconducting materials and insulators) over substrates. Magnetron sputtering has been widely utilized in preparation of thin films for electronic applications.

The principle of magnetron sputter deposition can be discussed by referring to the schematic diagram of sputtering process shown in Figure 2.2. High purity Ar gas is introduced as sputtering gas after evacuation of the chamber into low pressure. Due to the existence of electric field in the chamber, Ar gas is ionized and Ar ions bombard the target located on the magnetron resulting in ejection of atoms and ions from the surface of the target which in turn transfer and condense on the substrate in the form of thin films. As can be seen from the figure, magnets are attached to the target to effectively improve the sputtering process through confinement of the motion of secondary electrons emitted from the target in its vicinity leading to maintaining the plasma (creating more Ar^+) and then increasing the sputter yield [55].

2.4.1 Radio frequency Sputtering

DC sputter deposition of thin film from non-conducting targets such as, metal oxide and insulators cannot be practically implemented. This is because of the accumulation of the positively charged Ar ions on the non-conductive target which causes a shielding of the electric field and eventually stops the ejection of the atoms from the target surface (failure of sputtering process). To overcome this problem, RF sputtering process, in which alternating current with frequency of 13.56 MHZ is applied to the target can be used instead. By applying AC voltage, Ar ions would be accelerated towards the non-conducting target when it is negatively biased causing sputter out of

atoms from its surface [56]. However, when the polarity is changed the neutrality would be achieved. Similar to DC sputtering, the sputter deposition using RF sputtering can be carried out in reactive or non-reactive environment. In addition, unlike the DC sputtering, RF process can be used for both conductive and non-conductive targets.

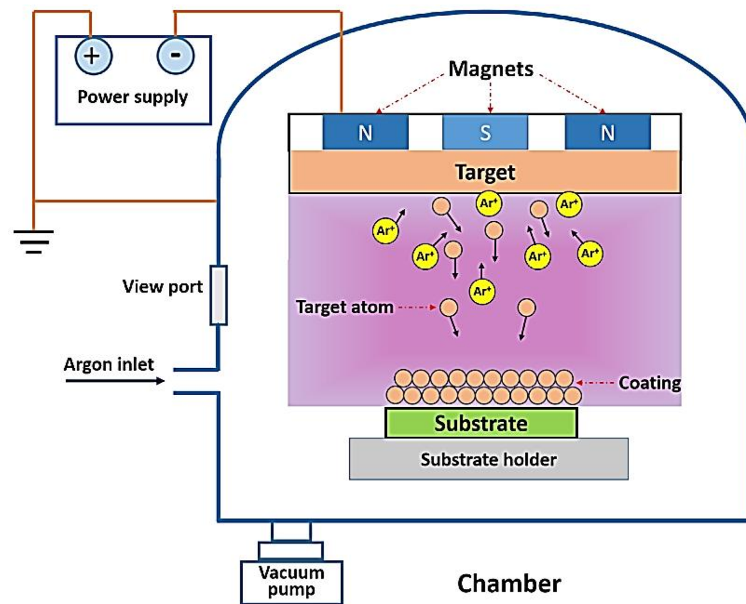

Figure 2.2. Schematic of magnetron sputtering process [57].

2.5 Growth of NiO Thin Films by Spin Coating: Review

Spin coating is a solution-based technique in which a sol-gel solution can be prepared and coated over a rotating substrate. In contrast to magnetron sputtering, which is an expensive and complex technique, spin coating is a simple and cost-effective technique to grow uniform thin films over large scale of substrate with good quality. The growth of NiO thin films by using sol gel spin coating at various growth conditions has been reported in the literature.

Nalage and co-workers [58] prepared NiO thin films through sol-gel spin coating technique. First nickel acetate tetrahydrate was dissolved in methanol and stirred at 60 °C for 1 hour, and then sintered at different temperature (400-700 °C) to

form NiO powders with different crystallite sizes. Second, NiO powders were put in m-cresol (3-methylphenol) solvent and stirred for 11 hours and then coated over glass substrate by spin coating. The films were analysed by XRD and it was found that when the sintering temperature was increased from 400 to 700 ^{o}C the crystalline quality of the films was improved. Moreover, the band gap of the films showed a decreasing trend with increasing the temperature (3.86 to 3.47 eV) which was attributed to enhancement in the crystallinity of the films.

Jlassi *et al*. [59] studied the effect of annealing temperature on the structural properties of spin coated NiO films. The films were coated on glass substrate at precursor molarity of 0.5 M and post-annealed at 300, 350, 400, 500 and 600 ^{o}C in atmospheric air for 1 hour. The study revealed that the films annealed at 300 and 350 ^{o}C did not show XRD diffraction peaks, indicating their amorphous structure; however, by increasing the temperature to 400 ^{o}C, a small diffraction peak correspond to (200) was observed. The further increase in the temperature to 600 ^{o}C led to appearance of new peaks which correspond to (111) and (220) plane. Moreover, the intensity of the diffraction peaks was increased and became sharper, suggesting improvement in the crystalline quality of the films.

Another work on the influence of the annealing temperature on the structural properties was reported by Liu's group [60]. They grew NiO films over SiO_2/Si substrate using sol-gel spin coating method. They observed that by increasing annealing temperature from 150 to 300, the films exhibited amorphous structure; however, when the temperature was increased to 350 ^{o}C, the film was crystallized and two diffraction peaks belonging to (111) and (200) lattice plane were detected. They also noticed that the amorphous films had low RMS surface roughness values, whereas the crystallized

film showed high RMS value due to the thermally derived grain growth that led to crystallization of the film.

The review of literature unveils that the physical properties of spin coated NiO thin films were affected by changing post-annealing temperature and precursor molarity. Srivastava *et al.* [61] reported that upon increasing the annealing temperature from 300 to 600 ^{o}C, the crystallite size of NiO films was increased from 14 to 18 nm and the band gap was decreased from 3.82 to 3.66 eV. On varying the molarity from 0.1 to 0.4 M, the crystalline quality was improved (the crystallite size was increased from 13 to 17 nm), whereas the energy band gap was decreased from 3.83 to 3.66 eV. They referred the decreasing trend in energy band gap with increasing the annealing temperature and molarity (increasing crystallite size) to the quantum confinement. Moreover, Turgut *et al.* [62] optimized the physical properties of NiO thin films coated on glass substrate through controlling the precursor molarity, annealing temperature, and the type of solvent. The molarity and annealing temperature were changed from 0.01 to 0.9 M and from 350 to 650 ^{o}C, respectively. 2-methoxyethanol, methanol and ultrapure water were chosen as solvent. The study revealed that NiO film prepared by using methanol as a solvent, molarity of 0.1 M and at annealing temperature of 550 ^{o}C showed the best crystalline quality with crystallite size, microstrain and lattice constant of 17.95 nm, 2.32×10^{-3} and 4.186 Å, respectively.

Recently, Xu and co-workers [63] investigated the influence of growth parameters (annealing temperature and precursor molarity) on the properties of NiO films. In their study, first NiO films were prepared using spin coating technique on glass substrate at fixed molarity (0.3 M) and the annealing temperature was changed from 150 to 500 ^{o}C. XRD results showed that the films annealed at temperatures below 300

^{o}C are amorphous, whereas the films annealed at 300 ^{o}C and higher temperatures revealed crystalline phase of NiO. The crystallite size was increased by increasing the temperature from 300 to 500 ^{o}C. The surface morphology analysis through SEM and AFM was also in line with the XRD analysis, whereby the films annealed at temperatures below 300 ^{o}C exhibited flat surfaces with low RMS surface roughness value, whereas the films annealed at 300 ^{o}C and higher temperatures showed growth of grains and increasing trend in RMS values. The energy band gap was decreased from 4.42 to 3.52 eV with increasing the annealing temperature. Second, the annealing temperature was fixed at 250 ^{o}C and the molarity was changed from 0.1 to 0.4 M. The change of molarity had no effect on the properties of NiO films. XRD results showed that all the films had amorphous structure.

Apart from growing NiO thin films over glass substrate, the growth of nanostructured NiO thin films on Si substrate using sol-gel spin coating technique has been reported in the literature. Turgut and his team fabricated heterojunction diode based on NiO/Si structure [64]. NiO thin film was coated over n-Si (100) substrate by spin coating technique at precursor molarity of 0.1 M and annealing temperature of 550 ^{o}C. XRD analysis revealed that the film had polycrystalline structure with preferred orientation along (200) plane. The crystallite size and the lattice constant were calculated as 23 nm and 4.184 Å, respectively. Paradia, *et al.* [65] prepared nanosheet NiO film on p-Si (100) using sol-gel spin coating route as photodiode. The photodiode was tested towards UV, red and green lights. Cavas [66] also prepared Li doped NiO film on n-Si (100) substrate using spin coating technique. The surface roughness and the energy band gap of the film were measured as 10 nm and 3.57 eV, respectively. The heterojunction was tested as a photodetector.

Table 2.3 shows the growth of NiO films using so-gel spin coating technique at different growth conditions over different substrates. Based on the survey of the literature and the summary on growth of NiO films by sol-gel spin coating presented in Table 2.3, it can be concluded that there is a lack of studies reported on the influence of growth parameters such as precursor molarity and annealing temperature on the physical properties of spin coated NiO films grown over Si substrate. Silicon substrate plays a key role in integrated optoelectronic devices due to its low cost and compatibility with electronic devices. Therefore, it is of high importance to investigate the growth of NiO thin films over Si substrate under different growth parameters by using a simple and cost-effective spin coating technique.

Table 2.3: Growth of spin coated NiO films on different substrate at different growth conditions.

Precursor/ Solvent/ Stabilizer	**Substrate type**	**Annealing Temp. (°C)**	**Molarity (M)**	**Crystallite size (nm)**	**E_g (eV)**	**Ref.**
Nickel acetate/ Methanol	No Sub. (Powder)	400 – 700	___	11 – 38	3.86 – 3.47	[58]
Nickel acetate/ Ethanol/ Monoethanolamine	SiO_2/Si	150 - 350	0.1	___	5.3 – 3.7	[60]
Nickel acetate/ 2-methoxyethanol/ Monoethanolamine	Quartz	300 - 600	0.5	14 – 18	3.82 – 3.66	[61]
	glass	400	0.1 – 0.4	13– 17	3.83 – 3.67	
Nickel acetate/ 2-methoxyethanol/ Monoethanolamine	Glass	500	0.01 – 0.9	13.3 – 12.7	3.75 – 3.42	[62]
		350 – 550	0.1 (optimum)	14.3 – 17.9	3.54 – 3.60	
Nickel acetate/ Ethanol/ Monoethanolamine	Glass	300 - 500	0.3	12.8– 36.4	3.68 – 3.52	[63]
		250	0.1 – 0.4	Amorphous	___	
Nickel acetate/ Methanol/ Monoethanolamine	n-Si (100)	550	0.1	23	3.74	[64]

2.6 Principle of Sol Gel Spin Coating

Sol-gel spin coating is a simple and effective route to grow thin films over flat substrates. Sol is a dispersion of colloidal particles in a solvent and it contains metal salts as precursors and some additives as stabilizers. Gel is a three-dimensional coherent network; therefore, sol-gel refer to the agglomeration of the colloidal particles in a form of continuous network. The process of preparing metal oxide films using sol-gel spin coating route is as follows;

i. Preparation of sol-gel solution through dissolving a metal salt such as nickel acetate tetrahydrate in a solvent and stirring the solution on hot plate until the solution becomes clear and homogenous. Adding the alkanolamine (R = MEA, DEA, TEA) as stabilizer to improve the stability and hydrolysis process of the solution.

ii. The resultant solution is aged to increase its viscosity and to make it in gel form, and then it is coated onto the substrate by spin coating unit. After that, the film is dried on a hot plate and then annealed at elevated temperatures.

Adding alkanolamine (R) to the Ni acetate precursor leads to the formation of Ni-R complexes which is thermally decomposed into nickel and hydroxyl ions during stirring on hot pate according to the following equations [67, 68];

$$\mathrm{Ni-R} \rightarrow \mathrm{Ni^{2+}} + 2\mathrm{OH^{-}} \quad (2.1)$$

The released Ni^{2+} and OH^{-} ions reacts with each other to form nickel hydroxide which can be decomposed into nickel oxide and water upon annealing at high temperatures as shown by Eqs. (2.2) and (2.3).

$$Ni^{2+} + 2OH^- \rightarrow Ni\,(OH)_2 \quad (2.2)$$

$$Ni\,(OH)_2 \xrightarrow{\Delta} NiO + H_2O \quad (2.3)$$

2.7 Review of Photodetectors based on NiO Thin Films

Multi-wavelength photodetectors (PDs) are of a great interest in a variety of applications such as imaging, medical treatment, astronomical observations, optical communication and military application due to their capability to detect multicolor light sources [69-73]. Low dimensional semiconductor nanostructures including Ga_2O_3, GaN, ZnO, TiO_2, CuO, CdS, and V_2O_5 have been utilized in UV and visible photodetection application due to their high surface area that enhances the photodetection properties. However, PDs based on these nanostructures are capable to detect only narrow spectral band [74-80].

In the past, NiO has been mainly used to fabricate p-n heterojunction UV PDs. Long *et al*. [81] prepared UV PD based on p-NiO/n-ZnO heterostructure and investigated its photodetection properties. The responsivity, rising time and falling time of the PD were found to be 2.23 mA/W, 20 s and 30 s, respectively upon exposure to 365 nm UV light at -5V bias. Huang and co-workers [82] demonstrated that n-SnO_2/p-NiO heterojunction shows good responsivity under UV light at -5 V bias with rising and falling times of 17 s and 9 s, respectively. Khun *et al.* [83] fabricated UV photodetector based on nanostructured p-NiO/n-TiO_2 heterojunction. The response and recovery time of the device were measured to be 0.1s under 365 nm UV light at 7 V bias. Zheng *et al* [84] fabricated n-type TiO_2 nanowells/p-type NiO mesoporous nanosheets heterojunction UV photodetector. The flower-like morphology of p-NiO nanosheets promoted active interfacial reaction sites to the exposure of UV light. This enhanced the generation of electron-hole pairs and thus high responsivity and sensitivity of